Effects of non-linearity and thixotropy in linear amplitude sweep testing for the evaluation of self-healing of bituminous binders

Materials and Structures (2024) 57:54
https://doi.org/10.1617/s11527-024-02332-y

ORIGINAL ARTICLE

Effects of non-linearity and thixotropy in linear amplitude sweep testing for the evaluation of self-healing of bituminous binders

Orazio Baglieri · Fabrizio Miglietta · Lucia Tsantilis · Ezio Santagata

Received: 14 September 2023 / Accepted: 11 March 2024

Abstract Linear amplitude sweep tests have been demonstrated to have good potential in being used for the evaluation of self-healing properties of neat and polymer-modified bituminous binders. Past research works, however, have neglected the effects of material non-linearity and thixotropy. This implies that the whole material integrity loss is attributed to damage and all restoration to self-healing, thus resulting in the possible overestimate of both damage and self-healing when evaluating the fatigue performance of materials. In the study described in this paper, specific experimental and analytical methods were adopted with the purpose of separating non-linearity and thixotropy in LAS healing tests. Non-linearity was assessed by means of multiple strain sweep tests carried out to determine the material non-linear viscoelastic moduli at specific testing temperatures. Thixotropy was considered by coupling self-healing LAS testing with a purposely defined test in which loading was applied to the undamaged material after a rest period equal to that applied in self-healing tests. Obtained results were processed by means of an analytical approach based on the simplified viscoelastic continuum damage model. Quantification of self-healing included the determination of material integrity and damage parameters recovered after the rest period. Such parameters, calculated by excluding time-dependent and non-linear biasing effects, can be used as straightforward indicators of the self-healing potential of neat and polymer-modified bituminous binders. Moreover, obtained results substantiate the concept that time–temperature superposition is still applicable when non-linearity is incorporated into the simplified viscoelastic continuum damage model.

Keywords Self-healing · Bitumen · Polymer-modified binder · Linear amplitude sweep · Non-linearity · Thixotropy · Simplified viscoelastic continuum damage model

1 Introduction

Bituminous binders are capable of self-repairing microstructural damage that occurs within the material due to external loadings and environmental conditions. Such a capability is referred to as self-healing [1]. Since self-healing is associated to the presence of microcracks, assessment of self-healing requires microcracks to be generated within the bituminous matrix so that the subsequent crack-closure process can be analyzed [2, 3]. This can be done by following different approaches, based on either fracture mechanics or fatigue. When considering fracture

O. Baglieri · F. Miglietta · L. Tsantilis (✉)
Department of Environment, Land and Infrastructure Engineering, Politecnico Di Torino, Turin, Italy
e-mail: lucia.tsantilis@polito.it

E. Santagata
Department of Civil and Environmental Engineering, Qatar University, Doha, Qatar

Published online: 03 April 2024

mechanics, the direct tension test, the ductility test, and the local fracture test are the most common protocols. Based on these methods, the fracture-dependent healing behavior can be studied in the presence of a visible crack [4]. For fatigue-based approaches, laboratory testing is typically done by subjecting binder samples to strain-controlled or stress-controlled loads by means of purposely devised methods such as the time sweep (TS) and linear amplitude sweep (LAS) tests. Both TS and LAS methods rely on the use of the dynamic shear rheometer (DSR) that is operated in the parallel plate configuration by employing small disk-shaped specimens [5–10]. TS tests, developed during NCHRP Project 9–10 with the purpose of evaluating fatigue failure of bituminous binders [11], involve the application of repeated cyclic strains or stresses with a prescribed constant amplitude and frequency. In strain-controlled mode tests, stress shows a decreasing trend because of the constant strain input, whereas in the stress-controlled mode, strain gradually increases during the test due to the imposed constant stress. In both strain-controlled and stress-controlled tests, specimens undergo progressive damage with a corresponding stiffness reduction, eventually reaching limiting conditions that can be identified by referring to several different criteria [12]. Although TS tests provide meaningful information pertaining to damage development, they are not included in the set of routine specification tests since they are very time-consuming and require multiple repetitions to attain good repeatability [13, 14].

The LAS test was introduced as an accelerated method to evaluate fatigue performance of bituminous binders [15]. The test procedure entails the material to be subjected to a shear strain input which is systematically increased to values high enough to expedite the damaging process. As a result, typical shear stress responses are characterized by a bell-shaped curve with a peak value of stress, after which stress decreases upon reaching ultimate failure. The LAS test has been standardized in AASHTO TP 101 [16].

Results of LAS tests can be processed by using the simplified viscoelastic continuum damage (S-VECD) model in its linear form [17, 18]. Such a model, based on Schapery's theory of work potential [19], is adopted to enable the prediction of fatigue life under any loading and temperature of interest using limited test results. However, the continuum damage model ignores the complicated microscale behavior of bituminous binders and quantifies damage evolution based on the effective stiffness reduction, without fully assessing the growth of microdefects.

LAS testing was recently adopted as a tool for the evaluation of self-healing properties of bituminous binders [20–22]. For this purpose, the standard LAS test procedure was modified through the inclusion of an intermediate unloading period between two loading phases. In the first phase, the test sample is loaded upon reaching specific values of shear strain amplitude in order to generate damage within the material matrix. In the second loading phase, which is prolonged until failure, the specimen is reloaded starting from an initial shear strain value equal to that imposed at the end of the first phase. During the intermediate period, the material is left idle for a preselected rest time to activate the self-healing process. As in the case of LAS tests, results of LAS-based healing tests are analyzed by means of the S-VECD model, adapted to include self-healing. In this regard, Xie and co-workers [23] quantified the healing potential of bituminous binders by successfully applying a rest-damage superposition principle with the purpose of constructing healing master curves of a damage-based parameter which accounts for rest period duration and damage level reached prior to rest. Construction of these healing master curves requires four different rest period durations and four damage conditions, thereby leading to sixteen tests in case of single repetition. With the purpose of shortening such a procedure, Wang and co-workers [24] proposed a simplified testing program by assuming that a single rest period duration is sufficient to assess healing potential for a given damage condition. Furthermore, these authors recommended the use of only three representative testing conditions for a full healing characterization. Proposing the application of rest-damage superposition in place of time–temperature superposition principle, Margaritis and co-workers [25] considered two other healing indices to construct the healing master curves. Such indices reflect the modulus recovery and the fatigue life extension due to the rest period, respectively. Other researchers suggested the adoption of different indices to evaluate healing. Asadi and co-workers [26] developed an index based on the decrease in crack length, consequently constructing healing master curves. Wang and co-workers [27] suggested that a parameter based

on the average stored pseudo strain energy, governed by strain amplitude, can effectively reveal intrinsic healing potential under various damage levels and rest periods.

It has been widely proven that the Schapery-type damage approach is capable of modeling the damage process of bituminous binders when the material is assumed to be linear viscoelastic (LVE) [13, 14, 17, 28]. However, appropriate considerations need to be made for non-linear viscoelasticity (NLVE). In fact, when the loading input exceeds the LVE limit, the proportionality between stresses and strains no longer holds. Therefore, the behavior tends to deviate from linear viscoelasticity, resulting in a softer and more viscous response [29, 30]. The main implication of such a simplified approach is the overestimate of damage since the whole stiffness loss is attributed to fatigue damage. To avoid such a misleading interpretation of test data, specific experimental procedures have been proposed to differentiate non-linear effects from those related to damage [31, 32]. They involve determining NLVE moduli of materials as a function of the loading input with the consequent possibility to incorporate non-linearity within the S-VECD framework [33–35].

Other phenomena, such as thixotropy, may interact with fatigue damage and self-healing mechanisms [36]. While self-healing involves the reversal of structural damage, thixotropy is related to the reversible time-dependent reorganization of material microstructure [37]. Thus, when the material is left idle after loading, the changes in its mechanical response are not exclusively related to the restoration of material integrity [38].

2 Research objectives

The primary objectives of this research work are:

- Evaluate the significance of non-linearity on the damage accumulation of bituminous binders during linear amplitude sweep testing;
- Assess the applicability of the time–temperature superposition principle within the non-linear framework of the S-VECD model;
- Consider the effects of time-dependent biases potentially occurring when rest periods are involved in the test timescale;
- Develop an expedite approach to quantify self-healing potential, by quantifying and removing the spurious effects of thixotropy and non-linear viscoelasticity.

3 Experimental investigation

Two unaged bituminous binders were considered for this experimental study. These are a 50/70 pen grade neat binder (N with a PG70-22), which was sampled from a refinery located in northern Italy, and a PMB 25/55–60 polymer modified binder (P with a PG76-22), containing a high percentage of styrene–butadiene–styrene (SBS) and produced in the plant according to an undisclosed processing scheme.

The two selected binders were subjected to rheological measurements which involved the use of a dynamic shear rheometer. All tests were carried out by means of the 8-mm parallel-plates geometry with a 2-mm gap between the plates. For each test type, a minimum of three replicates were performed and obtained results were averaged for subsequent analysis.

Experimental testing included three different test types: Temperature-Frequency sweep (T-f), Multiple Strain sweep (MS), and Linear Amplitude sweep-based (LA) tests. T-f tests were preliminarily conducted within the LVE threshold of the materials in small amplitude oscillatory shear conditions between 4 and 34 °C. MS tests were performed to exceed such a limit and to characterize the non-linear response in large amplitude oscillatory shear conditions. By referring to the LA-based tests, three different testing configurations were used with the purpose of investigating the material response to deleterious structural changes, in the presence of self-healing and by considering thixotropy. Such tests were indicated as the Standard LA (S-LA) test, the Repeated LA test (R-LA) test and Delayed LA (D-LA) test. Two values of temperature were considered for MS, S-LA, R-LA and D-LA tests. A first temperature of 20 °C was selected to represent a typical intermediate temperature. The second temperature, derived from the master curves of the norm of complex modulus, was used to guarantee equi-stiffness conditions, corresponding to 34 MPa. Equi-stiffness temperatures were found to be equal to 9 °C for binder N and 14 °C for binder P.

3.1 Temperature-frequency sweep tests

T-f tests were carried out to obtain the linear viscoelastic fingerprint of the bituminous binders. This required preliminary selection of the imposed strain amplitudes, according to the procedure described in previous works [39]. Such strain values ranged between 0.05 and 9% depending upon the considered temperature/frequency combination. Measurements were performed at test temperatures comprised in the range 4–34 °C (in steps of 6 °C, starting from 34 °C), by imposing a logarithmic variation of frequency from 100 to 1 rad/s at steps of 6 °C. Prior to measurements carried out at each temperature step, a thermal conditioning phase of 15 min was imposed to the specimen. Figure 1 displays typical input data and output results expressed in terms of angular frequency and norm of the complex modulus, respectively.

3.2 Multiple strain sweep tests

MS tests were carried out to investigate the nonlinear viscoelasticity of the bituminous binders. MS tests were performed at a fixed loading frequency of 10 Hz, and at temperatures set equal to those selected to perform the LA-based tests described in Sect. 3. Figure 2 displays typical input data of shear strain and output results expressed in terms of magnitude of the complex modulus normalized with respect to its initial value (herein indicated as normalized modulus). As highlighted in the graphs, a MS test is composed of two groups of measurements. Within each group, three successive blocks of logarithmic increments of strain amplitude are imposed to the material. Such strains are characterized by an initial minimum value, equal for both groups, and a maximum value dependent on the specific group. Initial strain amplitude was selected to be in the linear viscoelastic domain and was mainly dictated by equipment resolution. The maximum value of strain amplitude was set such that the linear viscoelastic threshold was overpassed only in the second group in order to explore the NLVE region of the binders. Initial strain amplitude values were selected to be equal to 0.1% whereas the final values were 1% and 10%, for group 1 and group 2, respectively.

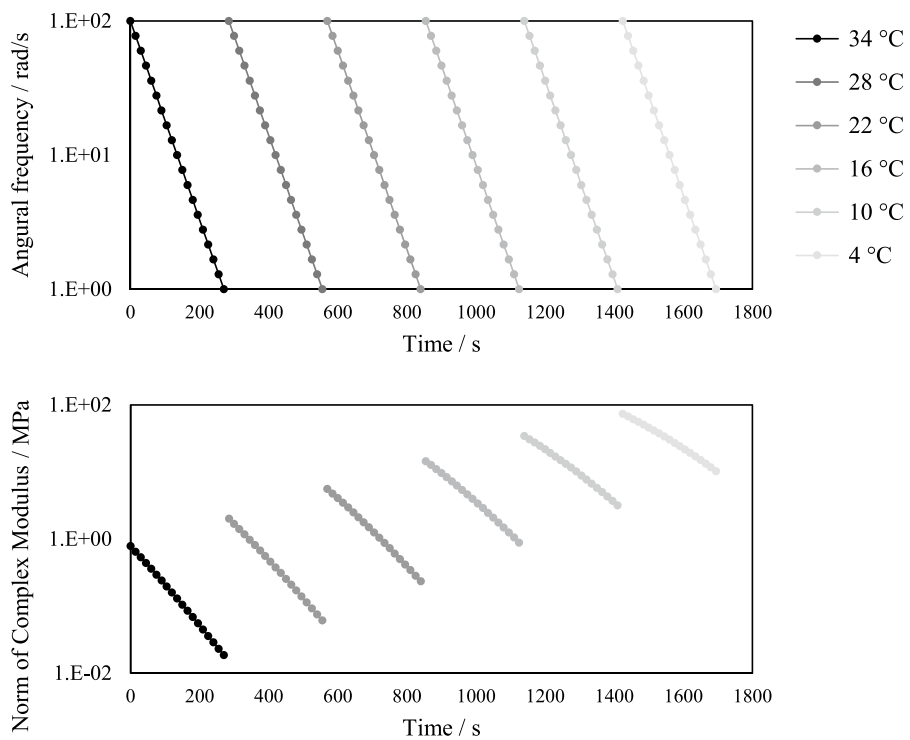

Fig. 1 Angular frequency and norm of complex modulus versus time from T-f test (binder N)

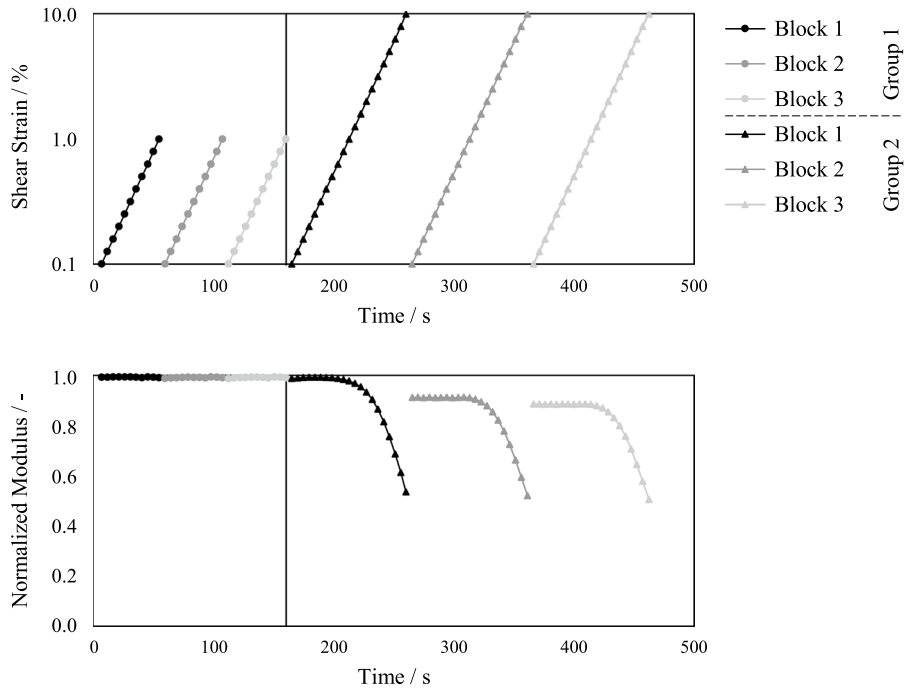

Fig. 2 Shear strain and normalized modulus versus time from MS test (binder N at $T = 20$ °C)

3.3 Linear amplitude sweep-based tests

LA-based tests were indicated as S-LA, R-LA and D-LA. Prior to each test type, a thermal conditioning phase of 30 min was always imposed to the specimen at the corresponding temperature of test (equal to 9 °C and 20 °C for binder N, and 14 °C and 20 °C for binder P).

3.3.1 Standard linear amplitude sweep tests

S-LA tests were conducted according to AASHTO TP 101 [16]. As per the reference protocol, tests start with an initial frequency sweep phase followed by a linear amplitude sweep step. The frequency sweep step is characterized by an increase of angular frequency, from 0.2 to 30 Hz, with an applied shear strain amplitude of 0.1%. The subsequent LA phase is conducted in the strain-control mode at a frequency of 10 Hz. The shear strain amplitude is increased in the stepwise mode starting from 0.1% up to 30%. Each step is characterized by an increment of 1% over 10 s. Figure 3 shows the loading pattern imposed to specimens during S-LA tests and the related shear stress output.

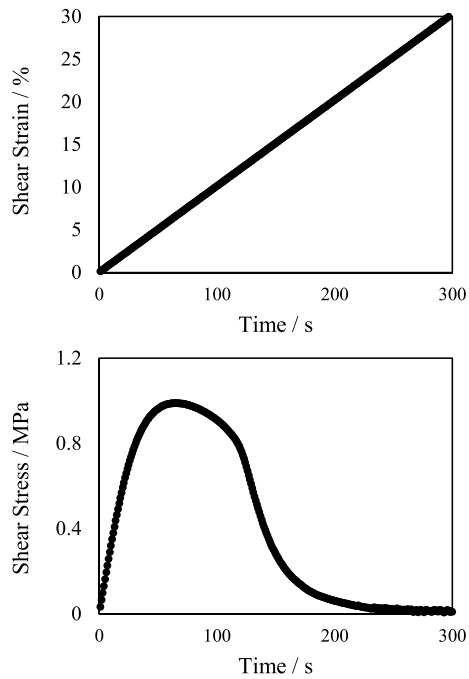

Fig. 3 Shear strain and shear stress versus time from S-LA test (binder N at $T = 9$ °C)

3.3.2 Repeated linear amplitude sweep tests

R-LA tests consist of two loading steps and an in-between rest phase. Two durations of the rest phase (thereafter labelled as t_{RP}) were considered, equal to 0 and 30 min. The value of t_{RP} equal to 0 min was intended to assess the damage conditions imparted to the specimen. Instead, the value of 30 min allowed restoration of material properties. For such a reason, in the case of t_{RP} equal to 30 min, material stiffness during the rest period was monitored by applying a value of continuous oscillatory shear strain equal to 0.1% at a frequency of 10 Hz, with data acquisition every 30 s. Typical input data and output results of such tests are showed in Fig. 4, in the case of rest period equal to 0 min and 30 min. As displayed in the figure, the first loading entails incremental strain amplitudes from 0.1% to the strain value corresponding to material failure gathered from S-LA tests. Definition of strain-related fatigue failure was identified by referring to the point of yield corresponding to maximum shear stress [12]. The second loading phase involved shear strain amplitudes increasing from 0.1 to 30% as in the case of S-LA tests. Both loading phases were applied at a frequency of 10 Hz.

3.3.3 Delayed linear amplitude sweep tests

D-LA tests consist of a S-LA test carried out after an initial rest period of the same duration of that imparted to the material during the R-LA tests (30 min). During the rest period, measurements were collected every 30 s by applying a value of continuous oscillatory shear strain equal to 0.1% at a frequency of 10 Hz, in order to monitor material stiffness. Such a test was introduced with the purpose of highlighting the possible hardening of the material, which may occur when it is left at rest. As documented in the literature [9, 35, 40], it is thought that such an effect can cause an overestimate of the restoration of material properties observed during the rest

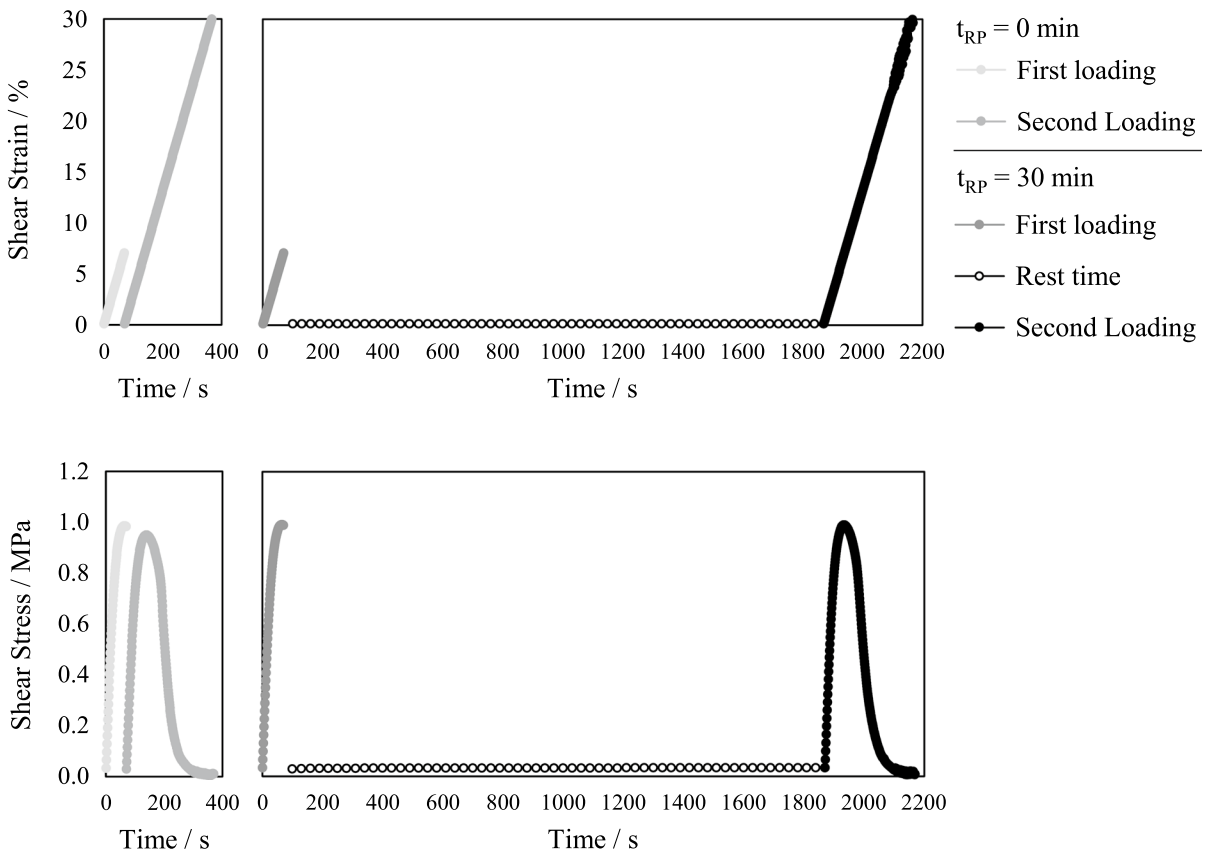

Fig. 4 Shear strain and shear stress versus time from R-LA test with t_{RP} = 0 min and t_{RP} = 30 min (binder N at T = 9 °C)

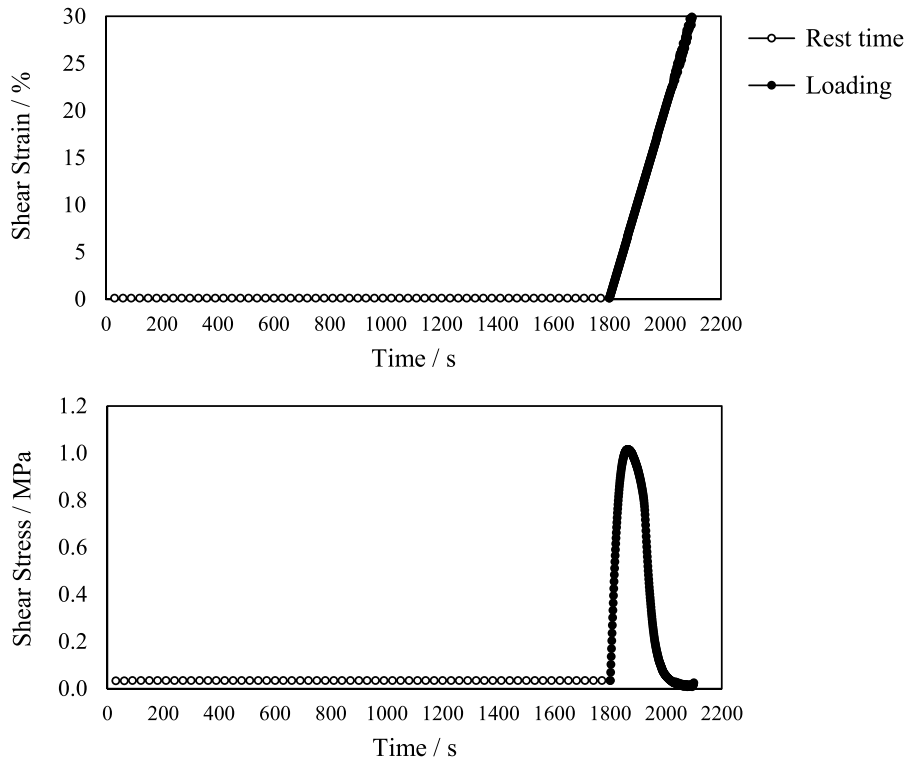

Fig. 5 Shear strain and shear stress versus time from D-LA test with t_{RP} = 30 min (binder N at T = 9 °C)

period as well as in the second loading phase of R-LA tests. Figure 5 illustrates, by way of example, the testing input and output.

4 Modelling

4.1 Linear viscoelastic modelling

The linear viscoelastic response needs to be modeled in order to apply Schapery's extended elastic–viscoelastic correspondence principle [41], with the subsequent calculation of pseudo-strains in the LVE domain. In particular, in the case of sinusoidal loading with zero mean displacement, as that applied in the DSR, pseudo-strains are evaluated by means of Eq. 1:

$$\gamma^{R}{}_{LVE} = \frac{1}{G_R} \bullet \gamma_p \bullet |G^*|_{LVE}(\omega, T) \tag{1}$$

where G_R is a modulus arbitrarily selected to be equal to 1, γ_p is the peak of shear strain, and $|G^*|_{LVE}(\omega, T)$ is the norm of complex modulus derived from its master curve.

Master curves of the binders were constructed by reducing measured linear viscoelastic properties (norm and phase angle of complex modulus) to a reference temperature by means of an optimization process which involved a simultaneous time–temperature (t-T) shifting and data fitting. The t-T shifting relied upon the William-Landel-Ferry (WLF) function, while fitting of data involved the Christensen-Anderson-Marasteanu (CAM) model [42, 43]. Equations of the CAM and WLF models are shown in Eq. (2) and Eq. (3), respectively:

$$\log|G^*|\left(\omega_R\right) = |G^*|_g \left[1 + \left(\frac{\omega_c}{\omega_R}\right)^{\frac{\log 2}{R}}\right]^{-\frac{mR}{\log 2}} \tag{2}$$

$$\log a_T = -\frac{C_1\left(T - T_R\right)}{C_2 + T + T_R} \tag{3}$$

where $|G^*|$ is the norm of the complex modulus, ω_R is reduced frequency, $|G^*|_g$ is glassy modulus, ω_c, R and m are CAM model parameters, a_T is the time–temperature shift factor, T_R is reference temperature, C_1 and C_2 are WLF model parameters.

4.2 Non-linear viscoelastic modelling

Non-linear viscoelastic response is included in the elastic–viscoelastic correspondence principle by means of the non-linear viscoelastic modulus of the material, the use of which allows damage-related effects to be discriminated from those related to non-linear viscoelasticity. In the case of sinusoidal loading with zero mean displacement, as in DSR testing, the non-linear viscoelastic solution for the pseudo-strain amplitude in each loading cycle at the applied frequency is given in Eq. (4) [33]:

$$\gamma^{R}{}_{NLVE} = \frac{1}{G_R} \bullet \gamma_p \bullet |G^*|_{NLVE}(\omega, T, \gamma_p) \tag{4}$$

where $|G^*|_{NLVE}(\omega, T, \gamma_p)$ is the non-linear viscoelastic modulus expressed as a function of the loading frequency, temperature, and shear strain amplitude.

Equation (4) indicates that non-linear pseudo-strains are equal to the predicted undamaged stress response (τ_p) corresponding to loading history divided by the reference modulus. This implies that, in the absence of damage, the non-linear viscoelastic response of the material is described by the elastic-like form of Eq. (5):

$$\tau_p = G_R \bullet \gamma^{R}{}_{NLVE} \tag{5}$$

4.3 Simplified viscoelastic continuum damage modelling

The S-VECD model is based on Schapery's theory of work potential employed to describe damage growth [19]. Such a phenomenon is quantified by means of the internal state variable S, derived from the rate-dependent damage evolution law given in Eq. (6):

$$\frac{\mathrm{d}S}{\mathrm{d}t} = \left(-\frac{\partial W^R}{\partial S}\right)^{\alpha} \tag{6}$$

where t is time, α is the undamaged material-dependent constant, assumed to be equal to $1/m + 1$, with m corresponding to the parameter of the CAM model of the norm of complex modulus (Safaei et al. 2016). W^R is the work performed, also referred to as pseudo-strain energy density, defined in Eq. (7):

$$W^R = \frac{1}{2}\tau \cdot \gamma^R = \frac{1}{2}C(S) \cdot \left(\gamma^R\right)^2 \tag{7}$$

where τ is the stress applied in a given cycle, and γ^R is the pseudo-strain. C represents the pseudo secant modulus that quantifies the integrity of the material, as expressed in Eq. (8):

$$C(S) = \frac{\tau}{\gamma^R \bullet MR} \tag{8}$$

where MR is the Modulus Ratio that takes into account specimen-to-specimen variability. This parameter, comprised between 0.9 and 1.1, is evaluated as shown in Eq. (9):

$$MR = \frac{|G^*|_{initial}}{|G^*|_{LVE}} \tag{9}$$

where $|G^*|_{initial}$ is the initial norm of complex modulus, given by the initial measured stiffness of the undamaged specimen under low strain conditions, and $|G^*|_{LVE}$ is the LVE modulus.

The combination of Eq. (6) and Eq. (7), via a numerical integration, leads to the definition of the internal state variable S, which represents the cumulative damage of the material at each time step i, as expressed in Eq. (10):

$$S_i = \sum_{i=1}^{N} \left(\frac{MR}{2} \bullet \left(\gamma^R\right)_i^2 \bullet \left(C_{i-1} - C_i\right)\right)^{\frac{\alpha}{1+\alpha}} \bullet \left(t_{R,i} - t_{R,i-1}\right)^{\frac{1}{1+\alpha}} \tag{10}$$

where t_R is the reduced time, evaluated as the ratio between the measured time and the time–temperature shift factor (a_T) determined from LVE characterization.

Although such a formulation allows the incorporation of temperature effects within the S-VECD framework [28, 44], it should be specified that it is a simplification to the fully rigorous S-VECD since the time varying function is not included.

The relationship between pseudo stiffness (or material integrity) and internal state variable (or damage parameter) is the core of the S-VECD model, known as the damage characteristic curve (DCC), and represents a material-dependent constitutive relationship.

Table 1 Parameters of master curves

CAM—WLF	N	P
$Log(G_g)$	2.93	2.84
$Log(\omega_c)$	2.06	1.60
R	1.82	1.67
m	1.11	1.02
C1	18.6	18.7
C2	149.4	145.9

5 Results

5.1 Linear viscoelasticity

Modeling of the LVE response of the binders as indicated in Sect. 4.1 led to the determination of the CAM parameters ($|G^*|_g$, ω_c, R, m) and WLF coefficients (C_1 and C_2) used for the construction of continuous master curves of the norm and phase angle of the complex modulus (expressed as a function of reduced angular frequency). The master curves model parameters, evaluated at the reference temperature of 20 °C, are listed in Table 1.

From the outcomes of the linear viscoelastic analysis, binder P was found to be characterized by a stiffness that was higher than that of binder N, as demonstrated by the values of the crossover frequency, ω_c, representing a measure of the material hardness. The master curve of binder P also showed a more gradual transition from elastic behaviour to steady-state flow, thus indicating a more rubbery and less brittle behaviour, as pointed out by the lower value of the rheological index, R. WLF coefficients were found to be quite similar, thus suggesting a similar thermal dependency of the selected binders.

5.2 Non-linear viscoelasticity

Non-linear viscoelastic features of considered binders were assessed by deriving NLVE moduli ($|G^*|_{NLVE}$) directly from the results of MS tests, represented as normalized values of the norm of the complex modulus plotted as a function of strain amplitude [39]. However, this required the results obtained in the three test blocks composing the second phase of testing (group 2) to be preliminarily compared among each other in order to highlight possible changes in response due to non-reversible permanent damage. For such a purpose, a vertical shifting of the curve of block 2 of group 2 was conducted to expand the viscoelastic representation beyond the LVE domain. Instead, as observed from test results, blocks 3 of group 2 led to minor damaging effects. Thus, any additional damage was assumed to occur only when higher levels of shear strain were imposed to the specimen. Healing effects were neglected since no rest periods were introduced between successive blocks. The vertical shifting process is displayed in Fig. 6, in terms of $|G^*|_{NLVE}(\omega, T, \gamma)$ normalized by $|G^*|_{LVE}(\omega, T)$ for binder P at 14 °C. The shifted curve is composed of an initial linear part within the LVE domain characterized by values equal to 1. When the shear strain is increased, the normalized modulus starts to decrease, thus revealing non-linearity. The reversibility of stiffness reduction observed by applying multiple repetitions of loading proved that such effects are caused by phenomena not related to damage. It can be pointed that, as expected, the extent of non-linearity was found to be both temperature and strain amplitude dependent.

Once $|G^*|_{NLVE}(\omega, T, \gamma)$ values were obtained, $\gamma^R{}_{NLVE}$ values could be determined by means of Eq. (4). The importance of discriminating non-linearity is exemplified in Fig. 7a, where the linear and non-linear cases of the pseudo-strains gathered from S-LA tests are compared. The area comprised between the two curves quantifies the impact of non-linearity which cannot be neglected when high values of loading inputs are imposed. Once non-linearity is removed from the analysis through the adoption of $\gamma^R{}_{NLVE}$, the incremental damage can be captured by plotting shear stress as a function of non-linear pseudo-strain as presented in Fig. 7b. It can be observed that when the

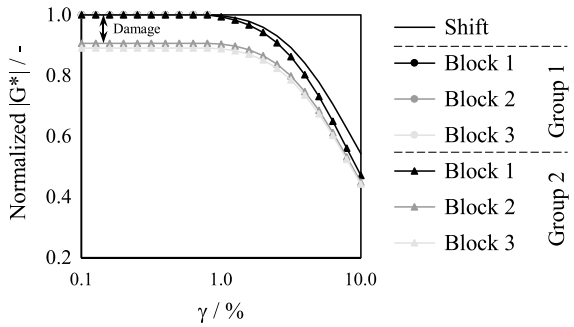

Fig. 6 $|G^*|_{NL}(\omega, T, \gamma)$ normalized by $|G^*|_L(\omega, T)$ (binder P at $T = 14$ °C)

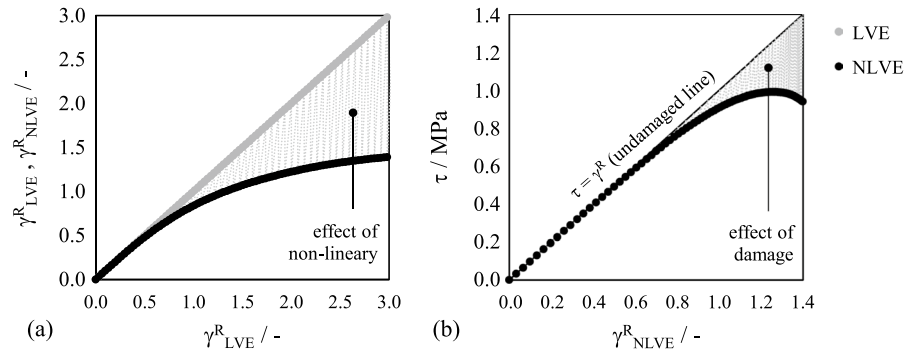

Fig. 7 Effect of non-linearity (**a**) and damage (**b**) (binder N at $T = 9$ °C)

non-linear curve collapses upon the identity line, no damage is occurring because shear strains are sufficiently low. Instead, deviation of the curve from the identity line depicts damage accumulation, as pointed out by the highlighted area. In both graphs, the curves are interrupted at a shear strain of 10%, corresponding to the maximum value investigated in MS tests.

The effect of non-linearity on the damage characteristic curves is highlighted in Fig. 8, where the curves were constructed by using LVE and NLVE pseudo-strains, in the case of binder N (a) and P (b). The curves refer to the analysis of S-LA data until peak shear stress. As observed from the figures, the LVE curves fall below the NLVE curves, with lower values of material integrity C and higher extension of the damage parameter S. This demonstrates that when non-linearity is not considered in the analysis, progressive damage is overestimated. When considering non-linearity, it can be observed that the NLVE curves fall above the LVE curves because the reversible component of non-linearity is removed, and the decreasing rate of the curves is dependent only on the effect of the damaging process. This highlights the importance of considering NLVE when performing the S-VECD analysis.

5.3 Time–temperature superposition

In the case of bituminous binders subjected to LA-based tests, applicability of the *t-T* superposition principle to the non-linear form of the S-VECD model needs to be verified. This requires the selection of a reference temperature (T_R) chosen to be equal to 20 °C. Afterwards, the DCC can be constructed at the T_R by accounting for temperature effects via the reduced time t_R, which introduces the time–temperature shift factors (a_T) determined from the linear viscoelastic characterization (as made explicit in the previous formulation of Eq. (10)). Thus, the construction of the DCC at the T_R translates into a shifting process of the DCC gathered at temperatures different from 20 °C ($T = 9$ °C for binder N, and $T = 14$ °C for binder P). It is implicit that the DCC gathered at 20 °C remains the same since it corresponds to T_R.

Results are displayed in Fig. 9 for binder N and P, without (a and c) and with (b and d) the application of the t-T equivalency. From the figures, it can be seen that the damage characteristic curves are unique to each binder, irrespective of temperature and that they are independent of material non-linearity. These results demonstrate the applicability of

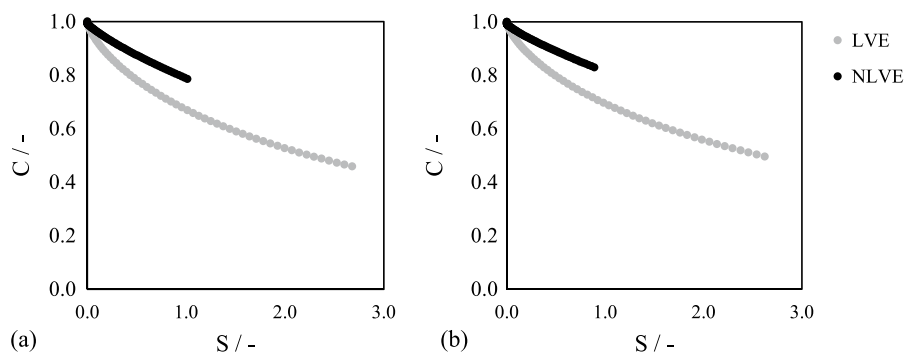

Fig. 8 Damage characteristic curves evaluated by considering LVE and NLVE behaviors (binder N (**a**) at $T = 9$ °C, and binder P (**b**) at $T = 14$ °C)

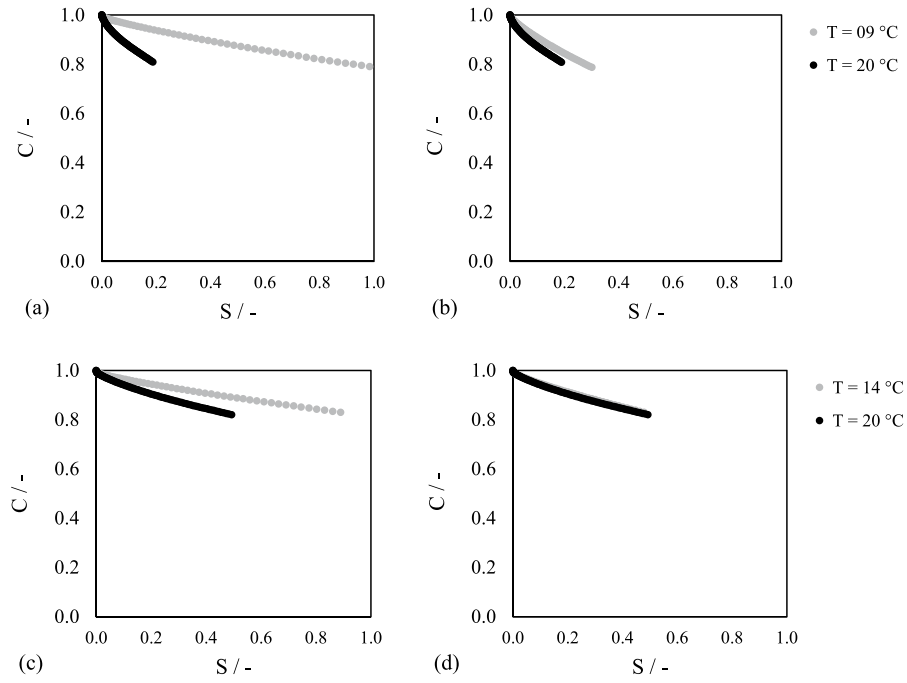

Fig. 9 Damage characteristic curves evaluated without (**a** and **c**) and with (**b** and **d**) the application of the *t-T* superposition principle at the $T_R = 20$ °C for binder N (**a** and **b**) and P (**c** and **d**)

t-T superposition to the non-linear solution of the S-VECD modeling.

5.4 Thixotropy

Thixotropy can cause an increase in stiffness that can be erroneously superimposed to that related to the self-repairing process, thus leading to an inaccurate interpretation of the self-healing capability of materials [35]. Figure 10a shows, by way of example, the isothermal increment of C_{RP} recorded during the rest period of D-LA tests in the case of binder N, at the two different temperatures (9 °C and 20 °C). In order to take into account such an increase in material integrity, the maximum increment in the C_{RP} values recorded at the end of the rest period (ΔC_{RP}) was considered as a correction factor. The factors ΔC_{RP} evaluated for the two considered binders are displayed in Fig. 10b. As expected, it is noted that such a factor is greater than one and tends to decrease as the testing temperature is higher, by a rate that is dependent on binder type.

The traditional S-VECD model, which does not consider thixotropy, can lead to an erroneous assessment of material integrity C, which also affects the state variable S since C enters in the formulation of S (Eq. (10)). Hence, Eq. (7) was corrected by means of the parameter ΔC_{RP} to account for the change in modulus caused by time-dependent phenomena occurring during rest periods.

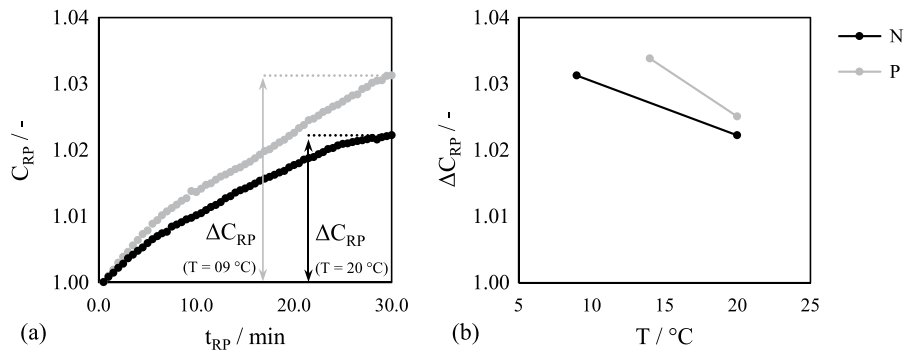

Fig. 10 C_{RP} values as a function of t_{RP} of D-LA tests (**a**) and factors ΔC_{RP} as a function of T (**b**)

Figure 11 displays the DCC curves obtained from S-LA and D-LA tests, before (a) and after (b) the correction by means of the ΔC_{RP} parameter. It is worth noticing that when the single loading phase is preceded by a rest period, the curve starts from a value that is greater than one (Fig. 11a), with a consequent overall shift of the curve. This outcome demonstrates the need to depurate results from time-dependent effects that take place during the unloading phase. As can be seen from the figure, the correction provided by ΔC_{RP} leads to an overlap between the DCC of D-LA tests and the reference DCC coming from S-LA tests (Fig. 11b).

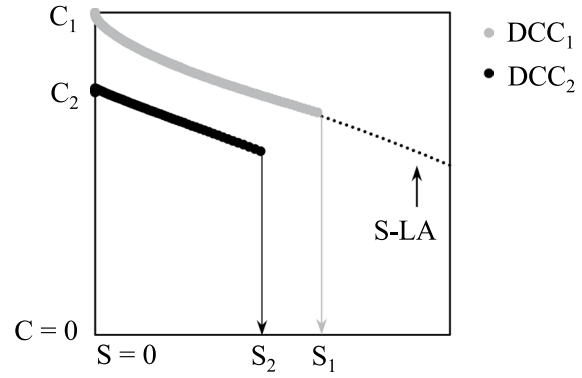

Fig. 12 Typical results of the analysis of R-LA data (binder N at $T = 20$ °C)

5.5 Self-healing

With the purpose of evaluating self-healing of the selected binders, the S-VECD model, in its non-linear form which includes the thixotropic parameter, was employed to interpret experimental data gathered from R-LA tests carried out with t_{RP} equal to 0 min (no rest period) and 30 min. The final formulations adopted in the analysis for the calculation of C and S are reported in Eq. (11) and Eq. (12), respectively:

$$C_{NLVE}{}'(S) = \frac{\tau}{\gamma^{R}{}_{NLVE} \bullet MR \bullet \Delta C_{RP}} \tag{11}$$

$$S = \sum_{i=1}^{N} \left(\frac{MR}{2} \bullet \left(\gamma^{R}{}_{NLVE}\right)_i^{2} \bullet \left(C_{NLVE}{}'_{i-1} - C_{NLVE}{}'_{i}\right) \right)^{\frac{\alpha}{1+\alpha}} \bullet \left(t_{R,i} - t_{R,i-1}\right)^{\frac{1}{1+\alpha}} \tag{12}$$

Typical damage characteristic curves corresponding to the first and second loading phases of a R-LA test (herein termed as DCC_1 and DCC_2) are displayed in Fig. 12, which refers to the no rest period condition ($t_{RP} = 0$). As expected, the DCC_1 overlaps with the reference DCC gathered from the S-LA test performed at the same temperature since it is independent of the rest period applied after loading. The DCC_1 eventually reaches the imposed damage level corresponding to peak shear stress, after which the binder is subjected to a new amplitude sweep. The subsequent DCC_2 is characterized by an initial value of C (C_2) and a terminal value of S (S_2) that are obviously different from those of the DCC_1. In particular, C_2 is lower than C_1 (equal to 1 as per definition of undamaged material), and S_2 is lower than S_1 (which can be reached at maximum accumulated damage).

Extending the analysis to the case of t_{RP} equal to 30 min, Fig. 13 shows the results obtained for binder N and binder P. Graphs on the left (a and c) correspond to the case of no rest period, whereas the ones on the right (b and d) refer to 30 min of rest.

In graph presented in Fig. 13a, c the difference between C_2 and C_1 is exclusively due to damage. The lower value of S_2 compared to S_1 is due to the

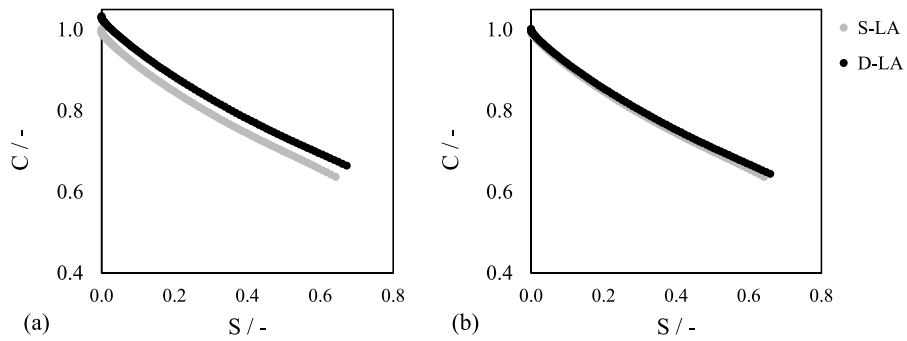

Fig. 11 Damage characteristics curves at $T_R = 20$ °C evaluated without (**a**) and with (**b**) the factor ΔC_{RP}

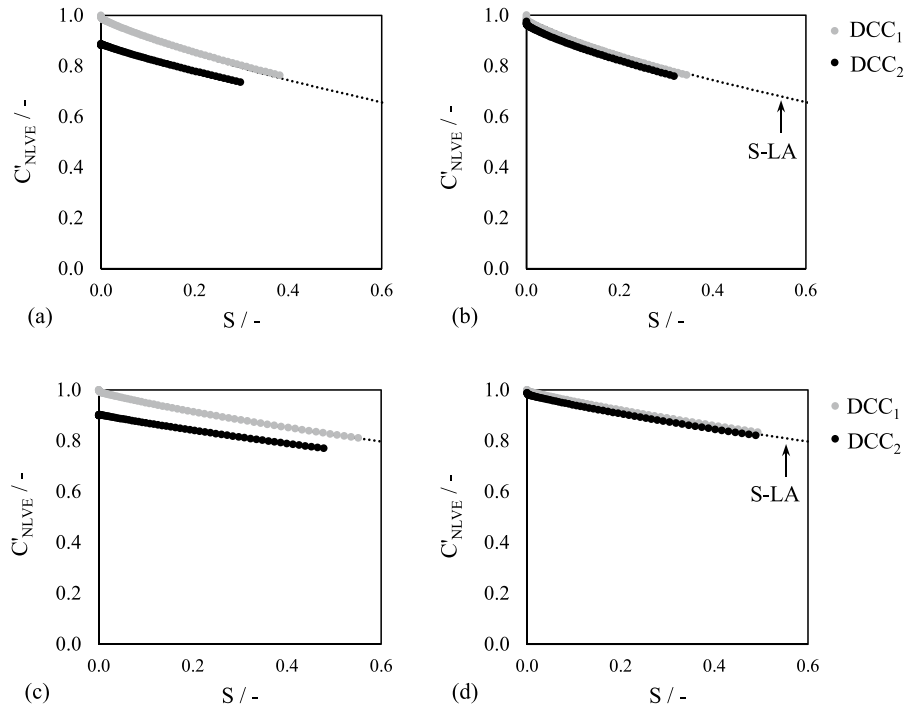

Fig. 13 Damage characteristic curves at $T_R = 20$ °C for binder N evaluated in the case of $t_{RP} = 0$ min (**a**) and $t_{RP} = 30$ min (**b**), and for binder P evaluated in the case of $t_{RP} = 0$ min (**c**) and $t_{RP} = 30$ min (**d**)

reduced capacity of the previously damaged material (S_2) to endure the same damage of the intact matrix (S_1). In the cases where a rest period is imposed (b and d), C_2 and S_2 tend to the values corresponding to the undamaged material (C_1 and S_1) as a result of self-healing effects. In other words, the closer the DCC_2 is to the corresponding DCC_1, the more the binder has been able to self-heal.

With the purpose of synthesizing damage and self-healing effects into simple parameters, the values of the ratios C_2/C_1 and S_2/S_1 can be considered for material integrity and damage, respectively. By referring to R-LA tests with no rest period, such values represent the imposed damage level corresponding to peak shear stress. This is the maximum deleterious structural change that can be healed by the binder. The longer the material is left idle, the greater is the self-healing achieved during rest and therefore such values can reach the maximum value of 1 without exceeding it. In the case of R-LA tests with rest periods, values of the abovementioned ratios are indicators of self-healing. Obtained values of such parameters are presented in Fig. 14 for material integrity (a) and damage (b), at the two testing temperatures.

By comparing the results, it can be noticed that C_2/C_1 values were always greater than S_2/S_1. Thus, C_2/C_1 seems to be more prone to reflect partial healing stages, thus leading to an overestimate of the true healing performance of binders. On the other hand, the parameter S_2/S_1 seems to be capable of quantifying the degree of full self-healing that occurs in the binder as a consequence of molecular interdiffusion and entanglement.

From a comparison of self-healing results, it can be noticed that each material shows a different self-healing capability, which is dependent on temperature. Binder P exhibited by far the greatest self-healing potential, reaching full healing at 20 °C. From a general overview of these results, the highest testing temperatures led to the highest values of healing parameters. For binder N, C_2/C_1 were quite similar at the two temperatures.

6 Summary and conclusions

The research work described in this paper proposes an expedite approach to quantify the healing characteristics of bituminous binders by adopting a testing protocol based on the linear amplitude sweep test. This new approach also accounts for the effects of thixotropy and non-linearity, that were properly

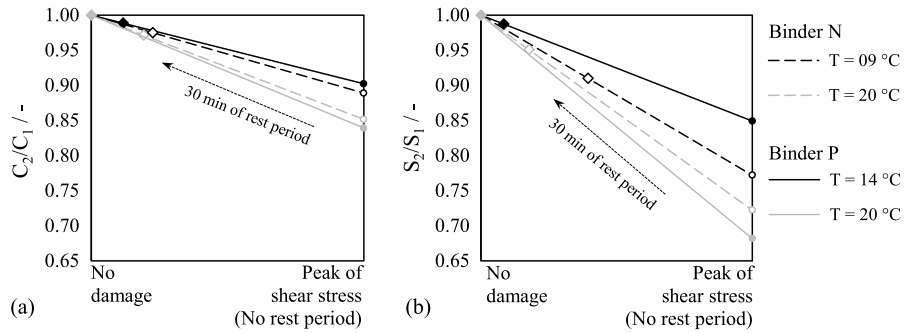

Fig. 14 Damage and self-healing parameters

embedded within the simplified viscoelastic continuum damage framework. The specific conclusions that can be drawn from this study are summarized as follows:

- Non-linear viscoelasticity needs to be considered in the overall analysis for an accurate prediction of damage and self-healing. For such a purpose, the multiple strain sweep test has been proved to be suitable to assess non-linear viscoelastic moduli up to approximately 10% shear strain amplitude, for the binders and testing temperatures considered in this investigation.
- Time-dependent effects due to thixotropy need to be quantified and removed from the overall observed response since it was found that they play a non-negligible role when rest periods are involved in the test timescale. For such a purpose, a specific correction factor was introduced within the modeling approach.
- The time–temperature superposition principle was found to be valid for the analyzed binders when non-linear viscoelasticity is introduced within the framework of the S-VECD.
- Modification of the standard linear amplitude sweep test was found to be suitable in evaluating the self-healing potential of bituminous binders by imposing a single rest period at the occurrence of fatigue failure, identified at peak shear stress. In doing so, two indicators of self-healing were defined based on the S-VECD-type material integrity gained and the damage accumulated after rest.

Obtained outcomes proved that the methodology yielded by this research work is able to capture the true damage and self-healing of bituminous binders, by eliminating the effects of thixotropy and non-linearity. Although such results are quite promising, the non-linear form of the S-VECD model used for self-healing assessment will be validated in the future by using a broader range of binder types and testing conditions (i.e. testing temperature, rest period duration and fatigue failure).

Funding Open access funding provided by Politecnico di Torino within the CRUI-CARE Agreement.

Data availability The raw/processed data required to reproduce these findings cannot be shared at this time as the data also forms part of an ongoing study.

References

1. Ayar P, Moreno-Navarro F, Rubio-Gámez MC (2016) The healing capability of asphalt pavements: a state of the art review. J Clean Prod 113:28–40
2. Santagata E, Miglietta F, Baglieri O, Tsantilis L (2020) Effect of temperature on self-healing properties of bituminous binders. In RILEM International Symposium on Bituminous Materials, Springer, Cham

3. Miglietta F, Tsantilis L, Baglieri O, Santagata E (2022) Investigating the effect of temperature on self-healing properties of neat and polymer-modified bituminous binders. Road Mater Pavement Des 23(sup1):2–15
4. Varma R, Balieu R, Kringos N (2021) A state-of-the-art review on self-healing in asphalt materials: mechanical testing and analysis approaches. Constr Build Mater 310:125197
5. Anderson DA, Le Hir YM, Marasteanu MO, Planche JP, Martin D, Gauthier G (2001) Evaluation of fatigue criteria for asphalt binders. Transp Res Rec 1766(1):48–56
6. Wang C, Zhang H, Castorena C, Zhang J, Kim YR (2016) Identifying fatigue failure in asphalt binder time sweep tests. Constr Build Mater 121:535–546
7. Sabouri M, Mirzaiyan D, Moniri A (2018) Effectiveness of linear amplitude sweep (LAS) asphalt binder test in predicting asphalt mixtures fatigue performance. Constr Build Mater 171:281–290
8. Baglieri O, Baaj H, Canestrari F, Wang C, Hammoum F, Tsantilis L, Cardone F (2020) Testing methods to assess healing potential of bituminous binders. In RILEM International Symposium on Bituminous Materials, Springer, Cham
9. Miglietta F, Tsantilis L, Baglieri O, Santagata E (2021) A new approach for the evaluation of time–temperature superposition effects on the self-healing of bituminous binders. Constr Build Mater 287:122987
10. Yan C, Yuan L, Yu X, Ji S, Zhou Z (2022) Characterizing the fatigue resistance of multiple modified asphalts using time sweep test, LAS test and elastic recovery test. Constr Build Mater 322:125806
11. Bahia HU, Hanson DI, Zeng M, Zhai H, Khatri MA, & Anderson RM (2001) Characterization of modified asphalt binders in superpave mix design (No. Project 9–10 FY'96)
12. Wang C, Castorena C, Zhang J, Kim YR (2015) Unified failure criterion for asphalt binder under cyclic fatigue loading. Road Mater Pavement Des 16(sup2):125–148
13. Hintz C, Velasquez R, Johnson C, Bahia H (2011) Modification and validation of linear amplitude sweep test for binder fatigue specification. Transp Res Rec 2207(1):99–106
14. Cao W, Wang C (2018) A new comprehensive analysis framework for fatigue characterization of asphalt binder using the linear amplitude sweep test. Constr Build Mater 171:1–12
15. Martono W, & Bahia HU (2008) Developing a surrogate test for fatigue of asphalt binders (No. 08–1356)
16. AASHTO (2018) Standard method of test for estimating fatigue resistance of asphalt binders using the Linear Amplitude Sweep. Washington D.C, AASHTO TP
17. Safaei F, Castorena C, Kim YR (2016) Linking asphalt binder fatigue to asphalt mixture fatigue performance using viscoelastic continuum damage modeling. Mech Time-Depend Mater 20(3):299–323
18. Baglieri O, Tsantilis L, Santagata E (2018) Evaluation of healing potential of bituminous binders using a viscoelastic continuum damage approach. Constr Build Mater 184:344–350
19. Schapery RA (1990) A theory of mechanical behavior of elastic media with growing damage and other changes in structure. J Mech Phys Solids 38(2):215–253
20. Aurilio M, Baaj H (2020) Examining the Effects of a self-healing elastomer on the properties of bitumen. In RILEM International Symposium on Bituminous Materials, Springer, Cham
21. Wang C, Xue L, Xie W, Cao W (2020) Investigation on self-healing of neat and polymer modified asphalt binders. Arch Civ Mech Eng 20(2):1–10
22. Yue M, Yue J, Wang R, Xiong Y (2021) Evaluating the fatigue characteristics and healing potential of asphalt binder modified with Sasobit® and polymers using linear amplitude sweep test. Constr Build Mater 289:123054
23. Xie W, Castorena C, Wang C, Kim YR (2017) A framework to characterize the healing potential of asphalt binder using the linear amplitude sweep test. Constr Build Mater 154:771–779
24. Wang C, Gong G, Chen Y, Sun Y (2022) estimating the healing characteristic of asphalt binder using the LASH test. J Mater Civ Eng 34(2):04021421
25. Margaritis A, Hasheminejad N, Pipintakos G, Jacobs G, Blom J, Van den Bergh W (2022) The impact of reclaimed asphalt rate on the healing potential of bituminous mortars and mixtures. Int J Pavement Eng 23(13):4664–4674
26. Asadi B, Tabatabaee N, Hajj R (2021) Crack-based healing master curve derived from linear amplitude sweep tests: a cohesive healing indicator for asphalt binders. Mater Struct 54(4):1–14
27. Wang C, Gong G, Ren Z (2023) Addressing the healing compensation on fatigue damage of asphalt binder using TSH and LASH tests. Int J Fatigue 167:107292
28. Safaei F, Castorena C (2016) Temperature effects of linear amplitude sweep testing and analysis. Transp Res Rec 2574(1):92–100
29. Anderson DA, Christensen DW, Bahia HU, Dongre R, Sharma MG, Antle CE, Button J (1994) Binder characterization and evaluation, volume 3: physical characterization. Strategic Highway Research Program, National Research Council, Washington, DC
30. Kim YR, Little DN (2004) Linear viscoelastic analysis of asphalt mastics. J Mater Civ Eng 16(2):122–132
31. Castelo Branco VTF (2009) A unified method for the analysis of nonlinear viscoelasticity and fatigue cracking of asphalt mixtures using the dynamic mechanical analyzer (Doctoral dissertation)
32. Underwood BS, Kim YR (2015) Nonlinear viscoelastic analysis of asphalt cement and asphalt mastics. Int J Pavement Eng 16(6):510–529
33. Underwood BS (2016) A continuum damage model for asphalt cement and asphalt mastic fatigue. Int J Fatigue 82:387–401
34. Safaei F, Castorena C (2017) Material nonlinearity in asphalt binder fatigue testing and analysis. Mater Des 133:376–389
35. Miglietta F, Underwood SB, Tsantilis L, Baglieri O, Santagata E (2023) Self-healing master curves of bituminous binders: a non-linear viscoelastic continuum damage framework. Road Mater Pavement Des 24(sup1):124–144

36. Sun D, Sun G, Zhu X, Guarin A, Li B, Dai Z, Ling J (2018) A comprehensive review on self-healing of asphalt materials: mechanism, model, characterization and enhancement. Adv Coll Interface Sci 256:65–93
37. Mewis J, Wagner NJ (2009) Thixotropy. Adv Coll Interface Sci 147:214–227
38. Leegwater G, Taboković A, Baglieri O, Hammoum F, Baaj H (2020) Terms and definitions on crack-healing and restoration of mechanical properties in bituminous materials. In RILEM International Symposium on Bituminous Materials, Springer, Cham
39. Tsantilis L, Underwood BS, Miglietta F, Riviera PP, Baglieri O, Santagata E (2021) Ageing effects on the linear and nonlinear viscoelasticity of bituminous binders. Road Mater Pavement Des 22(sup1):S37–S50
40. Santagata E, Baglieri O, Tsantilis L, Dalmazzo D (2013) Evaluation of self healing properties of bituminous binders taking into account steric hardening effects. Constr Build Mater 41:60–67
41. Schapery R (1984) Correspondence principles and a generalizedJ integral for large deformation and fracture analysis of viscoelastic media. Int J Fract 25:195–223
42. Ferry JD (1980) Viscoelastic properties of polymers, Third edition, Wiley
43. Marasteanu MO, & Anderson DA (1999) Improved model for bitumen rheological characterization. In: proceedings of the Eurobitume workshop on performance related properties for bituminous binders, 1–4
44. Chehab GR, Kim YR, Schapery RA, Witczak MW, & Bonaquist R (2002) Time-temperature superposition principle for asphalt concrete with growing damage in tension state. Journal of the Association of Asphalt Paving Technologists, 71